

SECTION TWO

Chapter Two

Motion Analysis and Biomechanics

by Robert W. Soutas-Little, Ph.D.

Dr. Soutas-Little is a Professor of Theoretical Mechanics and Director of both the Biomechanics Evaluation Laboratory and Biodynamics Laboratory at Michigan State University in East Lansing, Michigan.

INTRODUCTION

Classical, or Newtonian, mechanics is the oldest branch of physics devoted to the study of motion, the forces that cause that motion, and the internal forces that act within the body. Biomechanics is the application of Newtonian mechanics to the study of the neuromuscular skeletal system. Biomechanics has found its greatest use in orthopaedics and physical medicine and rehabilitation characterizing function and dysfunction of the muscular skeletal system. One branch of biomechanics, gait analysis or motion analysis of human gait, has developed since early studies in the late 1900s. Motion analysis has been extended during the past two decades to investigate many other activities in addition to gait analysis. Currently, postural balance studies, stair ascending, or descending, and upper limbs are all being studied using motion analysis and the techniques of biodynamics. Although motion analysis requires the use of the mathematical techniques of dynamics, the presentation here will be on a conceptual basis where possible.

TEMPORAL PARAMETERS OF THE GAIT CYCLE

There are variations in the definitions of the different phases of the gait cycle during walking but the most commonly defined phases will be discussed here.

The gait cycle is defined as the period from heel contact of one foot (for example, the left foot) to the next heel contact of the same foot. This cycle is broken into two parts, stance phase and swing phase. On the average, the gait cycle is about one second in duration with 60 percent in stance and 40 percent in swing. The stance phase is further divided into an initial double stance, followed by a period of single stance and then a final period of double stance. Double stance indicates that both feet are in contact with the ground; single stance is the period when only one foot is in contact with the ground. When walking, there must be a period of double stance and when running, this period is replaced by a flight phase during which neither foot is in contact with the ground. The walking gait cycle is illustrated in **Figure 1**. During the early part of stance phase, the heel is in contact with the ground, progressing to foot-flat during single stance and then to the forefoot contact during the final double stance phase ending with toe-off. This would be the normal contact areas of the plantar surface of the foot with the ground but may vary greatly with pathological gait. For example, equinus gait is characterized by the forefoot striking the ground first and then the contact area, progressing to the posterior in some cases while in others the heel never contacts the ground.

During double stance, the weight is transferred from one foot to the other. During single stance, the center of mass of the body passes over the foot in

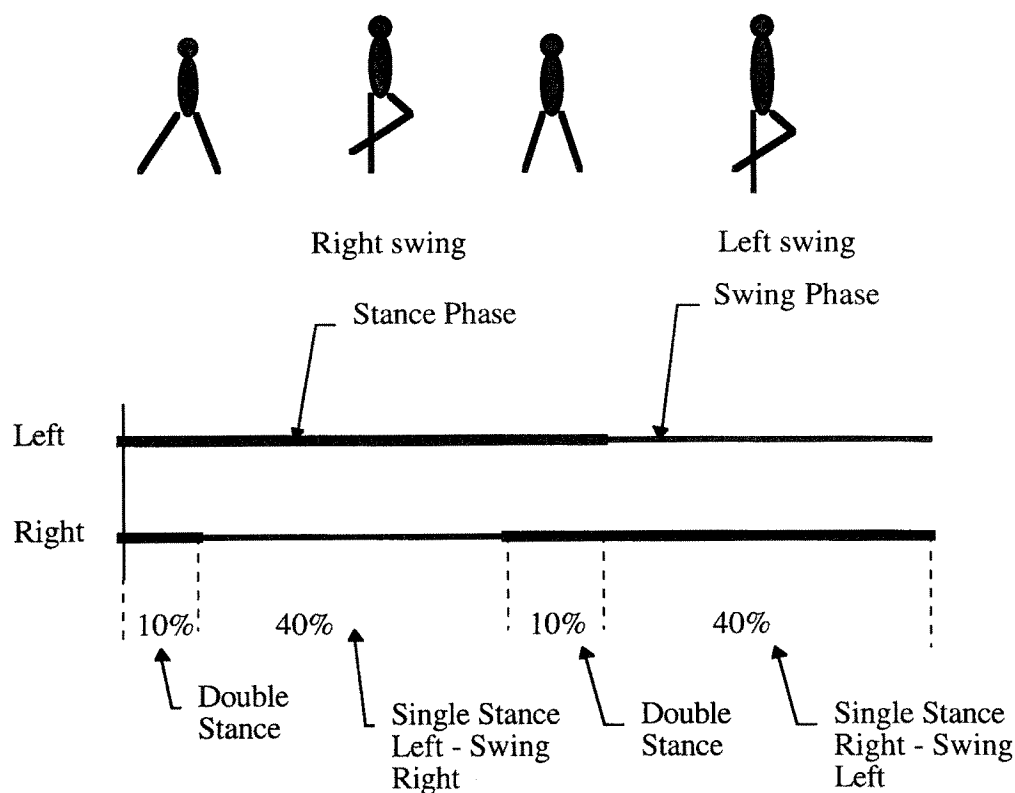


Figure 1 The Gait Cycle

Figure 1.
Temporal parameters of the gait cycle.

preparation for shifting to the other limb. Walking has been described as a series of falls from one limb to the other and it is obvious that the greatest danger of an actual fall is during this period of transferring weight.

BODY SEGMENTS

It is important to understand the basic assumptions that are made to analyze human motion using the techniques of rigid body dynamics. The most basic assumption is that body segments can be modeled as rigid bodies, that is, the position and motion of the underlying skeleton can be approximated by tracking the position and motion of the surface tissue. The error that arises is referred to as soft tissue motion error, which is inherent in all motion analysis of human

subjects. Only a few research tests have been performed to test the amount of error due to soft tissue movement and these tests have involved invasive techniques of putting pins in the bones and attaching markers to those pins and comparing pin marker movement with that of surface markers (1). Therefore, it is important to place surface markers at points where soft tissue movement is a minimum. Obviously, this can present problems when testing individuals who are obese.

When a body is modeled as a rigid body, the distance between any two points on that body is constant. Consider a body segment such as the thigh modeled as a single rigid body, as shown in **Figure 2**. Three markers are shown on the body segment so that they are non-collinear, that is, they do not lie on a line. The markers form a triangle on the body segment and it is assumed that the lines AB, BC, and CA do not

change in length. The position of each marker is measured by a motion analysis system and this position is expressed as coordinates in a fixed laboratory reference system. Different systems use different orientation of the laboratory coordinate systems but the method of analysis is the same for all systems. Consider the laboratory system shown in **Figure 3** and the position vectors to the three segment markers. We will define the three position vectors as:

$$\begin{aligned} \mathbf{r}_A &= X_A(t)\hat{\mathbf{I}} + Y_A(t)\hat{\mathbf{J}} + Z_A(t)\hat{\mathbf{K}} \\ \mathbf{r}_B &= X_B(t)\hat{\mathbf{I}} + Y_B(t)\hat{\mathbf{J}} + Z_B(t)\hat{\mathbf{K}} \\ \mathbf{r}_C &= X_C(t)\hat{\mathbf{I}} + Y_C(t)\hat{\mathbf{J}} + Z_C(t)\hat{\mathbf{K}} \end{aligned} \quad [1]$$

where $\hat{\mathbf{I}}, \hat{\mathbf{J}}, \hat{\mathbf{K}}$ are the unit base vectors in the laboratory coordinate system, that is, they are vectors of magnitude one that serve as pointers in the X , Y , and Z directions, respectively. Note that the components of each position vector are the coordinates of the marker position and are shown as a function of time as the marker position will change as the marker moves. This position is measured at specified intervals in time and this interval is dictated by the camera speed. The camera speed is usually specified in Hz (Hertz) or pictures per second. Therefore, a 100 Hz system would take 100 pictures per second or at intervals of 10 ms. As previously stated, the vector multiplying each component of the position vectors is the unit base vector of the laboratory system and may be thought of as a pointer of magnitude one pointing in the coordinate direction. These unit vectors form the basis of all vector analysis and are fundamental to the understanding of biodynamics. The laboratory coordinate system is a right-handed coordinate system, that is, the X axis is aligned with the thumb of the right hand, the Y axis is aligned with the index finger of the right hand and the Z axis is aligned with the middle finger of the right hand. All coordinate systems used in vector analysis must be right-handed coordinate systems (See **Figure 4**).

The position vectors to the three markers on the body segment will be used to obtain a segmental coordinate system, which may be thought of as three mutually perpendicular lines, attached to the body segment, that remain at a fixed orientation to that segment. In the discussion that follows, we will assume that the x segmental axis is in the anterior direction, the y segmental axis is in the medial-lateral direction directed to the left of the body segment, and the z segmental axis is directed in a superior direction on the body segment or directed distal to proximal in a lower

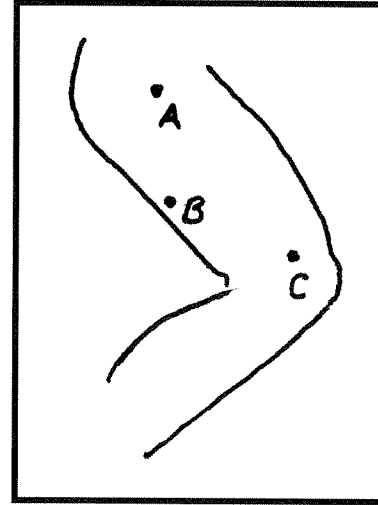


Figure 2.
Markers defining a rigid body segment.

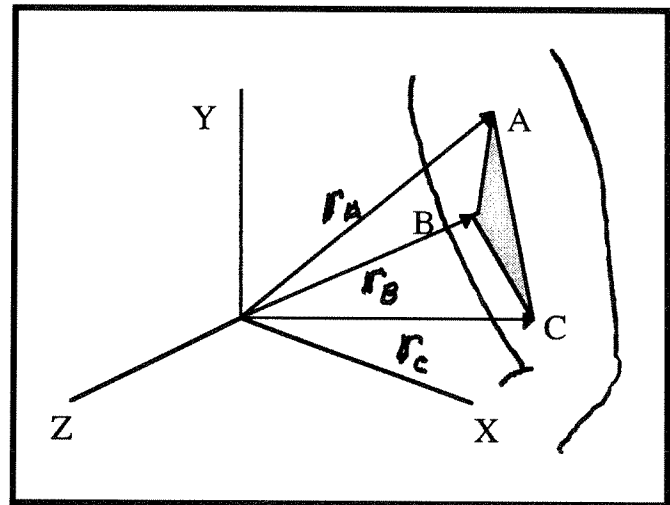


Figure 3.
Position vectors to body segment markers.

limb segment. Although there are many different ways to form the segmental coordinate system, we will assume for this discussion that the three markers have been placed on the body segment such that two markers define a segmental axis and the three markers form a segmental anatomical plane. For example, on the thigh, markers A and C may define the superior axis of the thigh and the three markers are placed in a parasagittal plane of the thigh. A relative position vector from C to A is designated by $\mathbf{r}_{A/C}$ (A relative to C) and is obtained

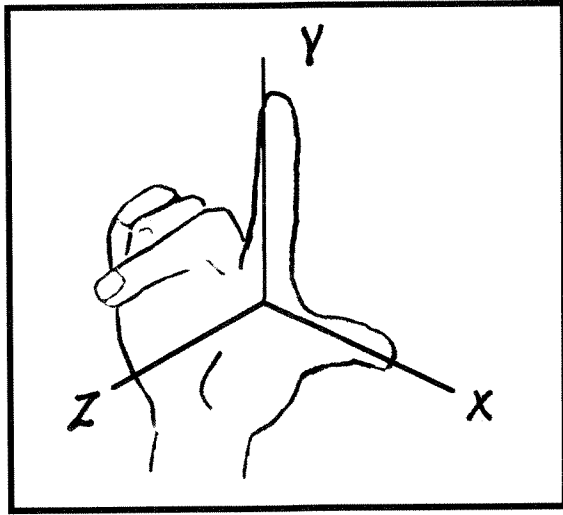


Figure 4.
Right hand coordinate system.

by subtracting the coordinates of marker C from those of marker A.

$$\mathbf{r}_{A/C} = \mathbf{r}_A - \mathbf{r}_C \quad [2]$$

It is important to realize that the length of this relative position vector does not change, since we have assumed that the body segment is rigid. The relative position vector may be thought of as a pencil glued to the body segment that is oriented with the body segment but does not change in length. If the length is computed on a frame-by-frame basis, the validity of the assumption may be measured. This length is called the magnitude of the relative position vector. A unit vector in the segmental coordinate direction z is obtained by dividing the relative position vector by its magnitude.

$$\hat{\mathbf{k}} = \frac{\mathbf{r}_{A/C}}{|\mathbf{r}_{A/C}|} \quad [3]$$

This unit vector will change its orientation in space but not its orientation relative to the body segment. A vector operation called the vector product, or cross product, is defined such that the resulting vector is perpendicular to the plane formed by two vectors. Let us form a second relative position vector from C to B

$$\mathbf{r}_{B/C} = \mathbf{r}_B - \mathbf{r}_C \quad [4]$$

If A, B, and C form a parasagittal plane, then a vector perpendicular to this plane in the medial-lateral direc-

tion can be obtained by taking the cross product between the relative position vectors defined in Equations 2 and 4 yielding a unit vector in the y segmental coordinate direction.

$$\hat{\mathbf{j}} = \frac{\mathbf{r}_{B/C} \times \mathbf{r}_{A/C}}{|\mathbf{r}_{B/C} \times \mathbf{r}_{A/C}|} \quad [5]$$

The final coordinate direction for the body segment is obtained by the cross product of the two segmental coordinate base vectors.

$$\hat{\mathbf{i}} = \hat{\mathbf{j}} \times \hat{\mathbf{k}} \quad [6]$$

The position of the body segment can now be determined by the position vector to marker C and the three-dimensional (3-D) orientation of the body segment is defined by the triad of segmental base unit vectors as shown in **Figure 5**. As mentioned earlier, there are many different protocols to place markers to define the segmental coordinate system but such a system must be formed for each body segment. Currently, there is no standard designation of which coordinate axis is oriented in which segmental direction. Here we have assumed that the x axis is in the anterior segment direction but some laboratories may designate the y or z axis in that direction. However, the segmental coordinate axes must be a right-handed coordinate system.

JOINT KINEMATICS

We have shown how the movement of a body segment can be tracked in the laboratory but what is of interest in the analysis of human movement is not the position and orientation (six degrees of freedom) of the

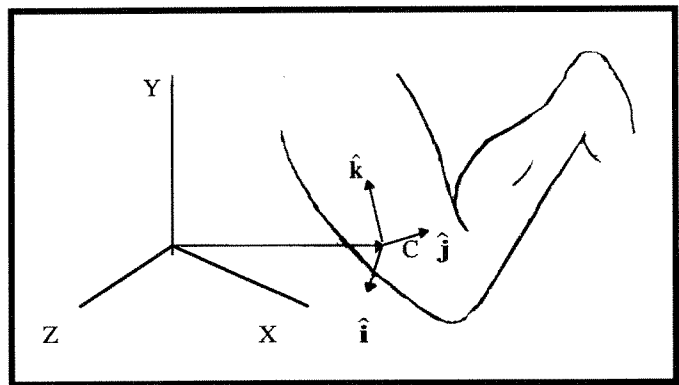


Figure 5.
Segmental coordinate system.

segment but the *relative* position and orientation of one body segment to the adjoining one; this describes the joint kinematics. The relative position of one body segment to another is easier to obtain but more difficult to interpret clinically so it will be discussed later. The relative orientation of one body segment to another defines the joint angles. For example, the orientation of the tibia to the femur defines the three clinical angles of flexion/extension, abduction/adduction, and internal/external rotation of the tibia relative to the femur.

Before we can define these clinical angles, we must consider finite 3-D rotations in general. It has been recognized for over 200 years that 3-D rotations are sequence dependent. This is illustrated in **Figure 6**; rotate a book 90° first about the x-axis (a)→(b) and then 90° about the y-axis (b)→(c). The order of rotations is then reversed: first rotate 90° about the y-axis (d)→(e) followed by a 90° rotation about the x-axis (e)→(f). This problem was first addressed by the Swiss mathematician Euler in 1776 (2). He recommended that rotations be defined by a sequence of three rotations. We will examine the knee joint angles defined by a sequence of rotations of the tibia relative to the femur

using a set of Euler angles suggested by Grood and Suntay (3) in 1983. We will represent the femoral coordinates with capital letters and the tibial coordinates with lower case letters. We will rotate first about the Y axis of the femur yielding the flexion/extension angle. The tibial x and z axes will no longer be parallel with the femoral X and Z axes and the tibial axes will be designated by x' and z' . The second rotation will be about the current tibial x' axis yielding the abduction/adduction angle. The tibial y' and z' axes will have rotated to a new position designated by y'' and z'' . The final rotation will be about the tibial z'' axis yielding internal/external tibial rotation. These rotations are illustrated in **Figure 7**. Note that the first rotation was about a femoral axis and the last rotation was about a tibial axis. The intermediate rotation is not about a current femoral or tibial axis but about an intermediate tibial axis. This is denoted as a Yxz rotation sequence, that is, rotation about the Y axis of the femur, followed by rotation about the intermediate x axis of the tibia and finally rotation about the z axis of the tibia. Euler (3) called this second axis the *line of nodes* and Grood and Suntay called it a *floating axis* (2). All joint analyses are

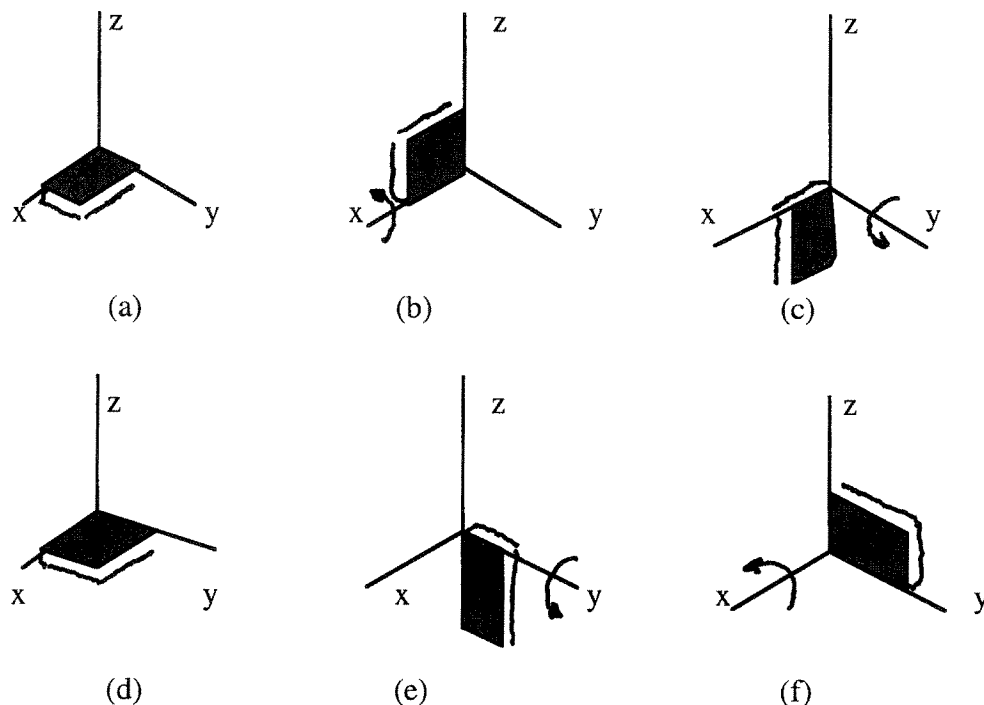


Figure 6.
Sequence dependence of finite rotations.

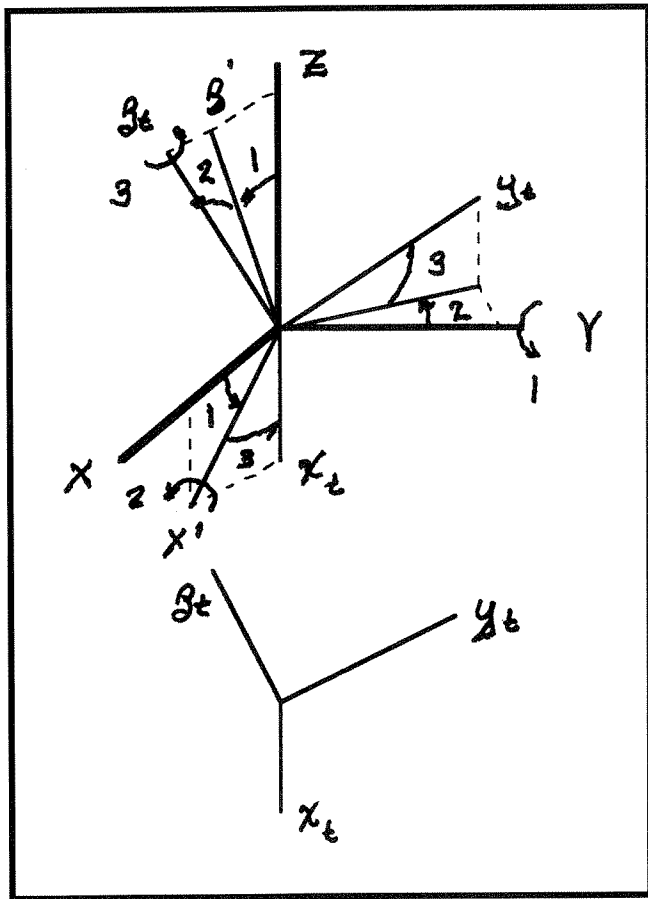


Figure 7.
Joint coordinate system.

based on a form of Euler angles. The difficulty is that different laboratory or motion analysis system manufacturers define the sequence of rotations in different orders, resulting in different joint angles. Care should be taken when comparison of data from one laboratory to another is made or in the interpretation of published data.

An example of the clinical importance of the sequence of rotations can be illustrated by examining head position relative to the thoracic cage. We will take the thoracic cage as the stationary or reference segment and examine head position relative to it. Examine two different sequences of rotations for the clinical interpretations of the motions. We will first do a (Yxz) sequence as was defined for the knee. Head flexion/extension will be defined as a rotation about the medial-lateral axis on the thoracic cage (the Y axis), followed by a rotation about the posterior-anterior head

axis at this intermediate position to obtain lateral side bending of the head and finally rotation about and inferior-superior head axis to define head rotation left or right.

Mathematically, we could alternately define the head position as a (Zxy) sequence. Head rotation left and right will first be defined by rotation about the vertical axis of the thoracic cage, followed by lateral side bending about the intermediate position of the anterior axis of the head, and finally, flexion/extension will be defined as a rotation about the medial lateral axis of the head. If you examine these two different definitions of the head angles, you will see that they are not only different in magnitude but in clinical interpretation. The question arises whether head flexion should be defined as a rotation about the medial-lateral axis of the thoracic cage or a rotation about the medial-lateral axis of the head regardless of the position of the head. It should be stressed that both are mathematically correct so that either is acceptable to the physical scientist. The clinical interpretation is whether cervical flexion and extension is predominantly motion in the lower or upper cervical spine segments. The first sequence argues that flexion/extension are primarily motions in the lower cervical spine and rotations left and right are motions in the higher cervical spine. The second sequence argues the reverse.

A more complex example of 3-D coupled motions is the shoulder joint. At the present time, only limited investigations have been made of this joint's motion and most of these have been cadaveric studies. Investigators at Mayo Clinic suggested a Zxz transformation sequence, that is, first circumduction about the vertical axis of the thoracic cage, followed by flexion about the current humeral axis (the floating axis), and finally internally or externally rotating about the distal/proximal axis of the humerus. This sequence of rotation was the one originally proposed by Euler in 1776 to describe the motion of a spinning top.

It is felt by most biomechanists that the choice of joint axes should be made on a joint-by-joint basis in order to give the most relevant clinical information. There have been attempts during the last few years to establish standard definitions but to date none have been established.

It is important to note that the coupling of the three joint rotations is very important clinically. Foot motion is frequently defined as pronation or supination, that is, a coupled motion of the ankle involving dorsiflexion, eversion, and medial rotation during pronation and

plantar flexion, inversion, and lateral rotation during supination. The motion of almost all joints cannot be described by simple two-dimensional (2-D) definitions.

Joint Center

If we are to discuss the moments or torques acting on a joint, we must define a point within the joint known as the joint center. For some joints, such as the hip, this point is easily defined from anatomical considerations. The hip joint is modeled as a ball and socket joint or, more precisely, a ball and half-socket joint. Therefore, the joint center is taken as the center of the spherical femoral head. The femur rotates about this point in movements of the femur relative to the pelvis and this point is stationary on both the pelvis and the femur. For other joints, there is not a clearly defined joint center. For example, the knee joint is characterized by the femur both sliding and rolling on the tibia and there is no single point that acts as a hinge point. We are then faced with the problem of defining an equivalent joint center. The easiest way is to define the geometric center of the joint as the joint center and this is set to be equal to the midpoint between the femoral condyles. Although this is certainly not the kinematic or rotational joint center, it will provide a reproducible reference point for the analysis of the joint moments.

It is possible to define a kinematic joint center using an *instantaneous center of rotation* for sagittal plane analysis or an *instantaneous helical axis* for general 3-D analysis. It is beyond the scope of this Chapter to discuss the mathematics to obtain these centers but the concept will be briefly presented. In a 2-D analysis of the motion of one rigid body relative to another, at any instant of time the two bodies rotate such that they appear to be hinged at a single point. At this instant, the velocity of this point will be the same if the point is assumed to be on the first or second rigid body. To understand this concept, we must first look at the linear velocity of a point on the rigid body and the angular velocity of the body.

Angular Velocity of a Body Segment

Consider two points on a body segment that is modeled as a rigid body as shown in **Figure 8**. The relative position vector $\mathbf{r}_{B/A}$ cannot change in length nor move on the body segment but may change orientation in space as the body segment rotates. In fact, this is how the rotation of the body is tracked. Points A and B have absolute linear velocities in space that are not, in general, equal. The linear velocity of a point is defined

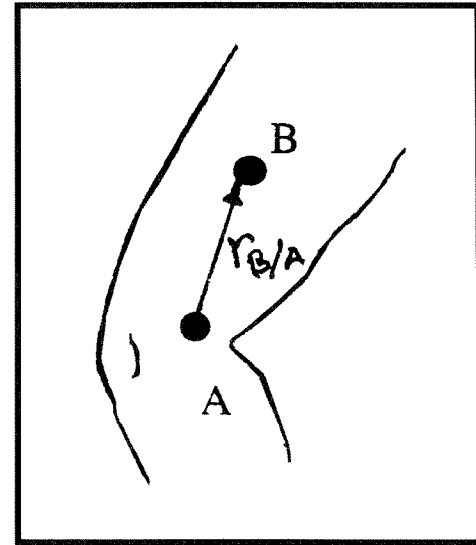


Figure 8.
Relative position vector.

as the time rate of change of the position vector to that point and the velocity is defined as the derivative of the position vector with respect to time as shown in **Figure 9**.

If we let $\Delta t = t' - t$, then the velocity is defined as

$$\mathbf{v} = \lim_{\Delta t \rightarrow 0} \frac{\Delta \mathbf{r}}{\Delta t} = \frac{d\mathbf{r}}{dt} \quad [7]$$

The relative velocity of point B to point A in **Figure 8** is defined as:

$$\mathbf{v}_{B/A} = \mathbf{v}_B - \mathbf{v}_A \quad [8]$$

Since the length of the relative position vector of B relative to A cannot change in length, the only thing that B may do relative to A is to rotate about it. This is fundamental to the definition of rotation of a rigid body or, in this case, a body segment. This relationship is expressed mathematically as:

$$\mathbf{v}_{B/A} = \boldsymbol{\omega} \times \mathbf{r}_{B/A} \quad [9]$$

where $\boldsymbol{\omega}$ is the angular velocity of the body measured in radians per second. (2π radians = 360°). The rigid body is said to have an angular velocity of $\boldsymbol{\omega}$ at this instant of time. The angular velocity is a vector having both a magnitude and a direction. The orientation of the vector is the axis of rotation and the sense is given by a right-hand rule, that is, if the thumb of the right hand is pointed in the direction of the vector, the fingers curl

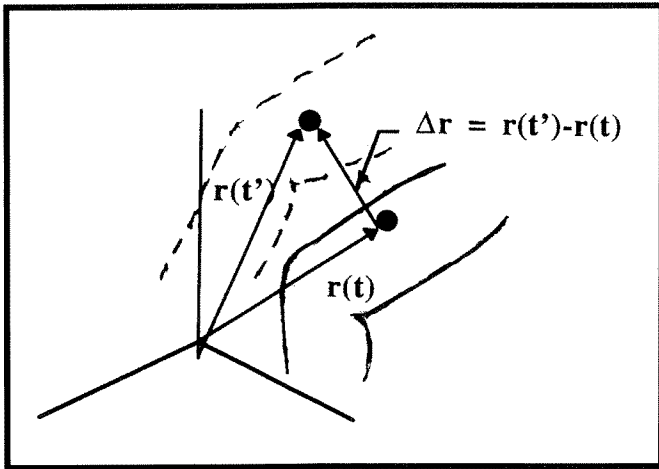


Figure 9.
Change in a position vector.

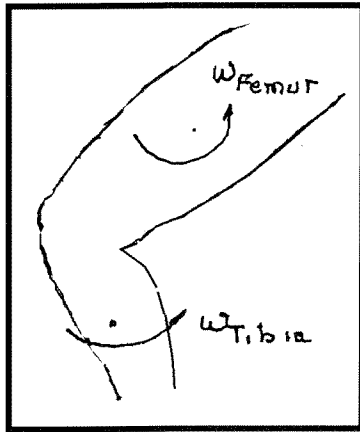


Figure 10.
Angular velocity of the knee joint.

around the vector and designate the rotation. The angular velocity vector designates the rotation of the body segment in an absolute sense (i.e., relative to the fixed laboratory coordinates).

The angular velocity of the joint is the relative angular velocity of the body segment distal to the joint relative to the proximal segment. Therefore, the angular velocity of the knee is:

$$\omega_{Knee} = \omega_{Tibia} - \omega_{Femur} \quad [10]$$

This is illustrated in **Figure 10**.

The angular velocity of the joint will have components in three directions and these components

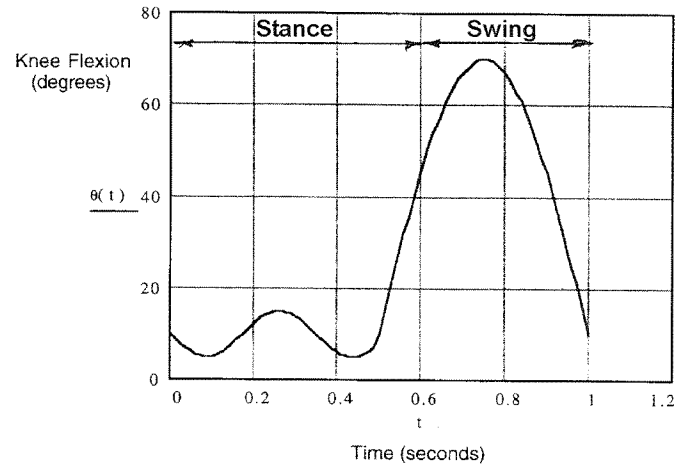


Figure 11.
Knee flexion for walking gait cycle.

will be equal to the rate of flexion/extension, abduction/adduction, and internal/external rotation. It is important to realize that the rate of change of a joint angle is different from the joint angle. For example, the knee may be flexed at a given time but be flexing or extending at the same time. If curve is plotted of the knee flexion/extension, the slope of this curve is the angular velocity component in flexion and extension. A typical flexion/extension curve for the knee is shown in **Figure 11**; the knee is approximately 10° flexed at heel contact and extends for the first 100 ms. This is followed by flexing and extending during single stance phase followed by flexing through toe-off to midswing. The final phase of swing is characterized by knee extension from the maximum flexed position. Note that the angular velocity of the knee in flexion and extension is the slope of this curve. If the slope is positive, the knee is flexing and if the slope is negative, the knee is extending. The maximum angular velocity of the knee occurs both during initial swing and late swing.

The concept of an instantaneous center of rotation or hinge point is a point on the femur that coincides with a point on the tibia that has the same velocity. When this concept is extended to three dimensions, one rigid body appears, at any instant, to rotate about an axis in space and to slide along that axis relative to the other body; hence, the term “instantaneous helical axis” or “screw axis.” Successive helical axes will intersect at points relative to the femur and the centroid of these intersections is defined as the joint center as shown in **Figure 12**. It is important to compare data

only as the definition of a particular joint center is the same in each analysis.

GROUND REACTION FORCES (GRF)

During gait, when the foot is in contact with the ground it applies a force to the ground and a GRF is developed that is equal and opposite to the force the foot applies on the ground. We are interested in this GRF because this is an external force acting on the body while walking. The only other external force acting on the body is gravitational attraction if wind resistance or drag is neglected. The force the foot applies to the ground is measured by a force plate or a dynamometer that is mounted securely in the floor such that its surface is flush with the floor (see **Figure 13**). The force plate has an instrument center that is below the floor and the resultant force and moment about this instrument center is measured. These data are sampled at a specific rate, usually 1000 Hz, or every millisecond. The resultant force and moment are expressed in an equivalent force system composed of the resultant force acting at a specific point on the surface of the force plate and a torque about the vertical axis. The resultant ground-reaction force is divided into three components: vertical, anterior/posterior, and medial/lateral. The torque is called the ground reaction torque and the unique point of the intercept of the GRF with the force plate surface is called the center of pressure (COP) or the center of force. The COP changes during stance phase generally moving from the rear of the foot anterior toward a point between the first and second metatarsal heads. The path of the COP on the force plate can be related to the path of the resultant ground-reaction force on the plantar surface of the foot. If an actual pressure distribution plot were obtained at an instant during stance phase, the COP would be the centroid of the pressure distribution. The COP path is also generated in this manner when pressure mats are used. Both pressure mats and force plates have been discussed in the Introduction.

Let us consider each component of the GRF separately; the largest is the vertical component and accounts for the acceleration of the body's center of mass in the vertical direction during walking. A typical plot of the vertical ground-reaction force is shown in **Figure 14** where the vertical reaction force is expressed in percent of body weight (%BW). This curve is sometimes called the **M** curve because it resembles that

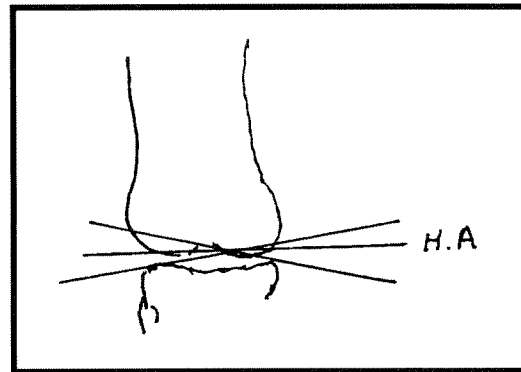


Figure 12.
Intercepts of helical axes (HA).

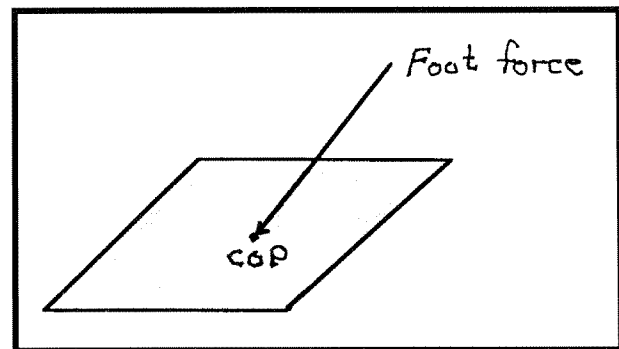


Figure 13.
Force plate and center of pressure (COP).

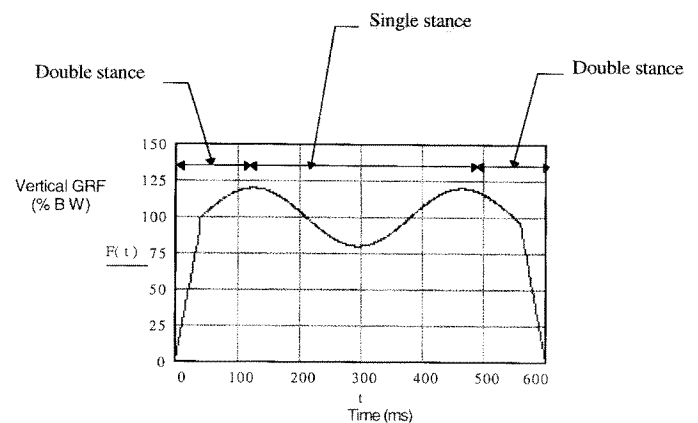


Figure 14.
Vertical ground reaction force (GRF) during walking.

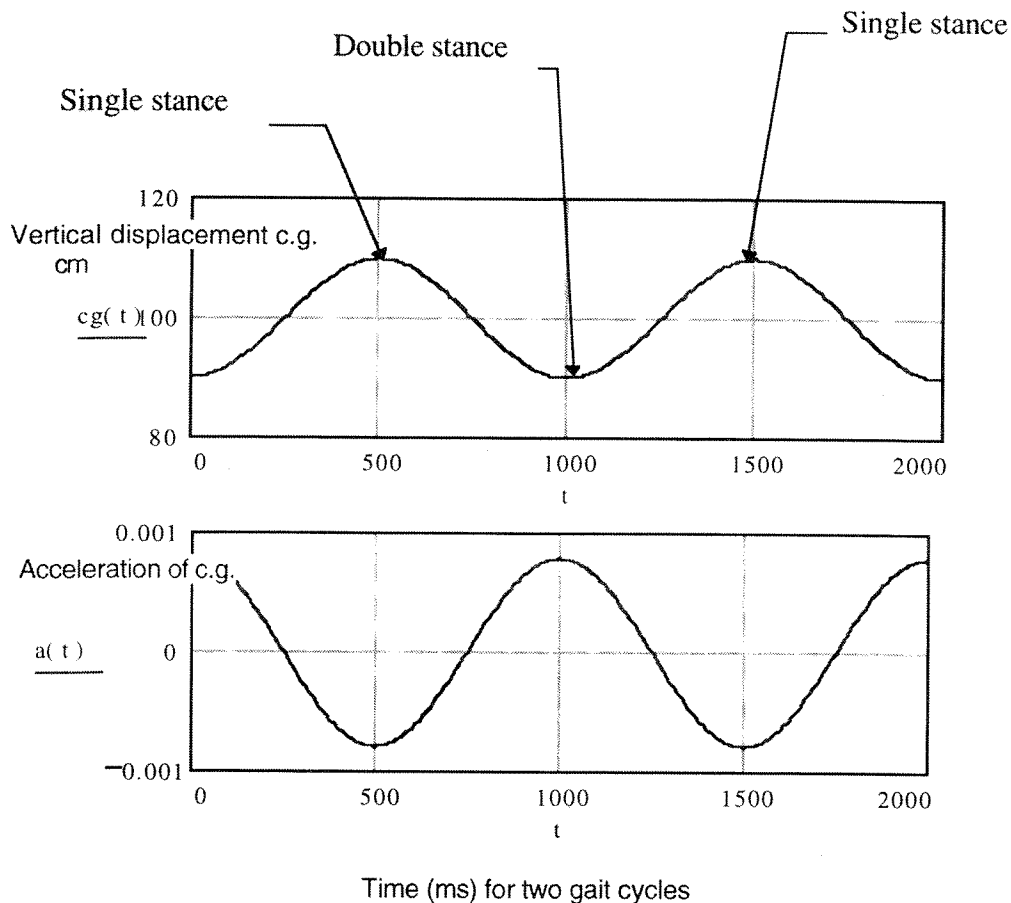


Figure 15.

Vertical displacement and acceleration of the center of gravity (c.g.) of the body during walking.

letter. During the first 100 ms, the GRF goes to a maximum of 120%BW during the double stance phase. During single stance phase, the vertical GRF drops to about 80%BW or for the more dynamic walker to 60 to 70%BW. At first, it seems unusual that the GRF should be less than body weight during single stance when only one foot is on the ground. This is made clearer if the vertical position of the center of mass of the body during the gait cycle is examined. The center of mass is located around the center of the pelvis, ignoring changes due to arm position, and executes a sinusoidal motion rising and falling about 10 cm in space during walking, as shown in **Figure 15**. The acceleration of the center of mass in the vertical direction is shown below the displacement of the center of mass and it can be seen that this is opposite in sign at each point in the

gaitcycle. If the entire body is treated as a mass on a spring, the magnitude of the GRF can be more easily understood. In **Figure 16**, the body is shown as a single mass and indicates the forces acting on the mass. Newton's second law states that the unbalanced force must equal the mass times the acceleration. Therefore, when the acceleration is positive, the GRF must be greater than BW. The positive acceleration occurs during double stance when the center of mass is at its lowest point. When the center of mass is at its highest point during single stance, the acceleration is negative and GRF must be less than BW. During a more dynamic gait, the vertical excursion of the center of mass is greater and vertical GRF will have a greater deviation from the BW. The GRF in the elderly remains at approximately BW during single stance.

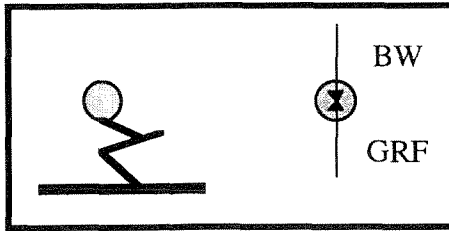


Figure 16.
Particle model of the body.

The anterior-posterior (AP) GRF is first a braking force to mid-stance, followed by propulsion, and usually represents a sine curve with an amplitude of 25%BW, as shown in **Figure 17**. The AP GRF is braking for approximately 50 percent of stance phase followed by propulsion. The area under any segment of this curve represents the impulse or the time integral of the force. The braking impulse should be approximately equal to the propulsion impulse for balanced gait left to right. The total impulse in the AP direction for a full gait cycle should be zero, as the impulse is equal to the change in momentum in the forward direction. If the individual is walking at a constant speed, there is no change in momentum and, therefore, no net impulse. If there is greater propulsion impulse on the left side as

compared with the right and greater braking impulse on the right as compared with the left, the net impulse for the complete gait cycle can still be zero. However, in this case, greater demands are being placed on the left leg to maintain a constant speed. This is seen frequently in cross-country runners after a stress fracture. The runner will be rehabilitated for a stress fracture on the right leg and returned to competition. However, the runner will be unbalanced in function, placing higher demands on the left leg. If this state is allowed to continue, it usually results in a stress fracture of the uninjured leg due to the higher functional demands placed on that leg. All cases of this nature should be tested on the force plate and balanced by a trainer when necessary. The unbalanced AP force is compared with normal as shown in **Figure 18**.

The medial-lateral force is of lower magnitude in most situations and relates to balance during walking. The medial-lateral GRF initially acts in the medial direction with a magnitude of 10%BW or less and then acts laterally during the balance of stance phase.

The vertical ground reaction torque has received much less attention in gait analysis but is felt to be involved in the pelvic twist and arm swing during gait. It also has been used as a balance measurement in postural balance studies.

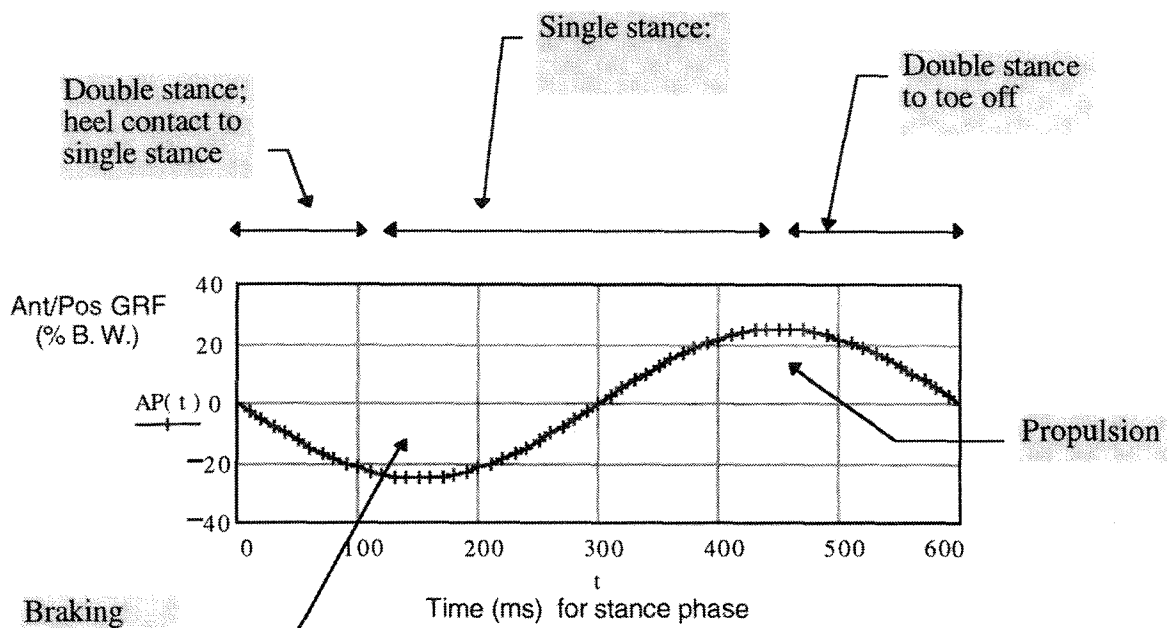


Figure 17.
Anterior-posterior (AP) ground reaction force (GRF).

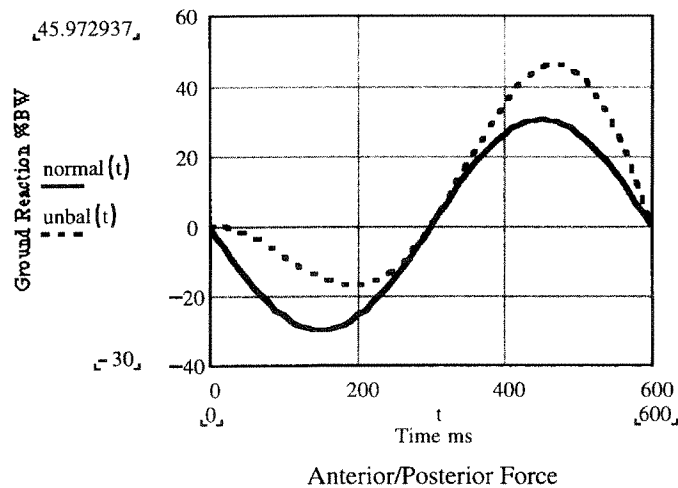


Figure 18.

Anterior-posterior ground reaction force for normal subject and subject with unbalanced limb.

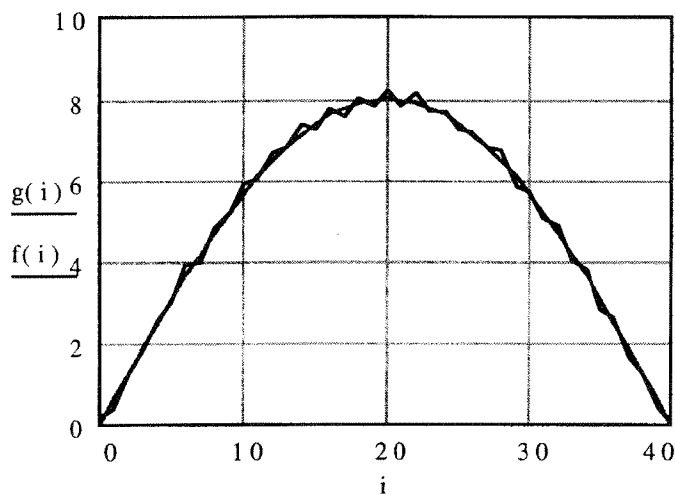


Figure 19.

Noise in position data.

KINETIC STUDIES

In most engineering studies of dynamics, the direct dynamics problem arises, that is, the forces are known and are used to develop the differential equations of motion. These equations are usually nonlinear in nature and numerical solutions are sought. The solution involves integration of the equation; a process, which by its nature, smoothes out noise in the force data. On the other hand, most biodynamics problems involve the inverse dynamics solution, wherein the motion of the

body is known and the forces are obtained by differentiation of the position-time curves. Mathematically, this is an easier process if the position is known as a continuous function of time. However, as has been discussed in the Instrumented Gait Analysis Section and also in this Chapter, motion data are not obtained as continuous functions of time but at discrete intervals depending upon the speed of the video cameras. The forces and moments are then obtained by differentiation of these data. Since analytical differentiation cannot be used, the data must be differentiated numerically.

For an example of the inverse dynamics problem, consider that the displacement given is the function of time as:

$$x(t) = \sin(\pi t) e^t.$$

The velocity and acceleration are obtained by successive differentiation of this function:

$$\begin{aligned} v(t) &= e^t [\sin(\pi t) + \pi \cos(\pi t)] \\ a(t) &= e^t [2\pi \cos(\pi t) + (1 - \pi^2) \sin(\pi t)]. \end{aligned}$$

In this case, the position was given analytically as a continuous function of time.

Modern motion analysis equipment allows measurement of position data from 50 to 200 times a second (frame rates 50–200 Hz) using high-speed video cameras. This means that the position data are not known as a continuous analytical function but at discrete times. Higher frame rates can be obtained for use in measurements of high velocity movements. As previously noted, most experimental systems do not collect position data as a continuous function of time but at specific intervals of time. The velocity and acceleration are obtained by numerical differentiation of these data and are thus subject to increased noise in the calculation of the velocity and acceleration. As an example, suppose that the correct position function is

$$g(t) = 8 \left[\sin \frac{\pi t}{40} \right]$$

and the position datum $f(t)$ has noise of a random nature and maximum magnitude of 0.3 units as shown in **Figure 19**. These are not actual data but a file created using a random number function. Now we numerically differentiate both $g(t)$ and $f(t)$ to see the effect of the noise on the differential. The differentiated functions $dg(t)$ and $df(t)$ are shown in **Figure 20**. It is clearly seen in this file that the differentiated data are too noisy to be reliable. To completely describe the motion, the data

would have to be differentiated a second time to obtain acceleration. In actual practice, the position data are filtered using digital filters to smooth the data and to obtain more reliable differentiation in the presence of noise. Numerical differentiation techniques and digital filters are beyond the scope of this Chapter but the user of any motion analysis system should be aware of what types of differentiation and filtering routines are used.

Once the data have been filtered and differentiated, the joint forces may be obtained by solving from the most distal segment proximally. Each segment is modeled as a rigid body and isolated from the other segments but shows all forces acting on the segment—a free-body diagram; an example is shown in **Figure 21**. In this case, the GRF and the segment weight (W) are known and the ankle joint force (JF) and moment (M_a) are sought. The Euler-Newton equations of motion for a rigid body are:

$$\sum \mathbf{F} = \frac{d\mathbf{p}}{dt} \quad [11]$$

$$\sum \mathbf{M}_{c.m.} = \frac{d\mathbf{H}_{c.m.}}{dt}$$

where \mathbf{p} is the linear momentum of the segment and is equal to $m\mathbf{v}$, that is, the product of the mass of the segment and the velocity of the center of mass of the segment and where $\mathbf{H}_{c.m.}$ is the angular momentum of the segment about the center of mass. The angular momentum is equal to:

$$\mathbf{H}_{c.m.} = I_{xx}\omega_x \hat{\mathbf{i}} + I_{yy}\omega_y \hat{\mathbf{j}} + I_{zz}\omega_z \hat{\mathbf{k}} \quad [12]$$

where the I 's are the mass moments of inertia about the segmental coordinate axes. The mass moment of inertia is a measure of resistance to the angular acceleration about each coordinate axis. Values of the mass, location of the center of mass and the mass moments of inertia are available in the literature. The right side of Equation 11 is known and these algebraic equations can be solved for the joint force and moment. The proximal joint force and moment on the next is solved in a similar manner now that the distal joint force and moment for this segment are known.

The Euler-Newton equations of motion given in Equation 11 can be expanded into six scalar equations. Three equations for the linear momentum yielding:

$$\begin{aligned} \sum F_x &= ma_x \\ \sum F_y &= ma_y \\ \sum F_z &= ma_z \end{aligned} \quad [13]$$

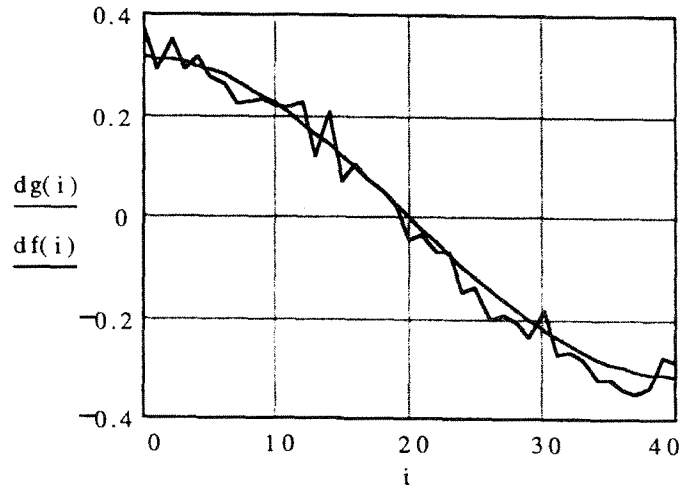


Figure 20.
Noise in velocity data.

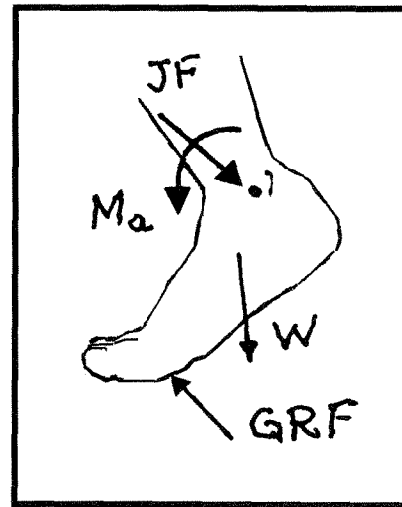


Figure 21.
Free-body diagram of foot.

The three equations for the angular momentum are more complex, yielding:

$$\begin{aligned} \sum M_x &= I_{xx}\alpha_x - \omega_y\omega_z(I_{yy} - I_{zz}) \\ \sum M_y &= I_{yy}\alpha_y - \omega_z\omega_x(I_{zz} - I_{yy}) \\ \sum M_z &= I_{zz}\alpha_z - \omega_x\omega_y(I_{xx} - I_{zz}) \end{aligned} \quad [14]$$

The right-hand side of Equations 13 and 14 are known from motion analysis data and the forces and moments

at the proximal joint of the segment are determined by solution of these simultaneous equations.

Quasi-static Determination of the Joint Moments

In many cases, during slow walking, stair ascending or descending, or mild squatting, sufficient accuracy during stance phase can be obtained by ignoring the right-hand side of Equations 13 and 14. These terms are called the inertial forces, or inertia terms, and depend upon the linear and angular acceleration of the body segments. Especially during stance phase of gait, these terms are small compared to the GRFs, and the joint forces are calculated from the GRFs only. We may get a conceptual idea of the joint moments by examining **Figure 22**.

Figure 22 is not meant to be an exact representation of the location of the joint centers or the GRFs at some moment during gait but will give an example as how quasi-static moments can be determined. Although there are formal methods to determine the moments at any joint center using vector algebra and are used in most clinical software packages, the concept of sagittal plane joint moments may be obtained from this simple figure. The GRF has been shown as two separate

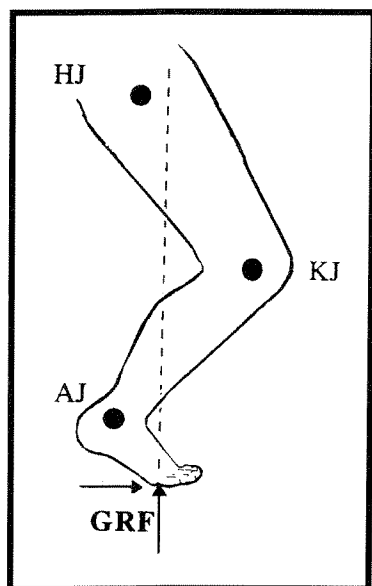


Figure 22.

Joint centers and line of action of ground reaction forces (GRF). AJ (ankle joint), KJ (knee joint), and HJ (hip joint).

components, one acting in the anterior direction and the second in the vertical direction. The simplest definition of a moment is the magnitude of the force times the perpendicular distance from the joint center to the force, that is:

$$M = F d \quad [15]$$

Examining the ankle joint represented by the ankle joint center, we can see that both the anterior GRF and the vertical reaction force produce an applied or external dorsiflexion moment. If the ankle is not to collapse, the muscle moment must be equal and opposite to the applied moment. Therefore, there must be a net plantar flexion muscle moment or the gastrosoleus complex must produce the dominant muscle activity.

At the knee joint, the vertical GRF is a knee *flexion* force while the anterior GRF would cause knee *extension*. It is not obvious which of these applied moments will dominate since the vertical GRF is larger but has a lower moment arm (perpendicular distance from the joint) while the lower anterior GRF has a greater moment arm.

At the hip joint, both the anterior and vertical GRFs produce applied flexion moments, which must be resisted by the hip extensors. At first, this may appear to be a simple method to determine the dominant muscle activity at any joint. However, this is compromised by the fact that many muscles are two joint muscles producing opposite reactions at each joint (e.g., the hamstrings are hip extensors and knee flexors). This does give a feeling of the antagonistic muscle activity.

A similar view of the moments in the frontal plane can be obtained by examining **Figure 23**; wherein the net GRF passes medial to the knee center and causes an applied knee adduction moment during all of the stance phase of gait. If the individual is suffering from medial knee pain, each step aggravates this condition. If this moment is the cause of the pain, it is easy to determine by asking the individual to rotate his/her foot laterally, thus reducing the moment arm of the force from the joint center.

Body Segments Considered as Levers

The easiest way to begin to understand the forces produced by the muscles spanning a joint and, therefore, the loads that are applied to the joints, is to consider simple levers, as shown in **Figure 24**. For this system to be in equilibrium (static balance), the total force acting on the lever must be zero and the turning effect, or the moment of the forces about the fulcrum *C* must be zero. These two conditions may be written as:

$$F_C = F_A + F_B$$

$$F_A a = F_B b \quad [16]$$

Note that since the moment arm to F_b is greater than the moment arm to F_a , the force at A must be bigger than the force at B to balance the moments or the turning effects of the forces. This can affect the loads on the spine when an individual is lifting an object. The fulcrum point of the lever model of a lifting motion is the spine, in this case a point on the lumbar spine, and a lever model is shown in **Figure 25**. One can take some typical values of the weights lifted and the weight of the torso and compute the force that the posterior back muscles must resist. If the individual is lifting 50 lb and the upper portion of the body is 120 lb, the moment arms to the weight, the center of mass of the torso, and to the back muscles, may be estimated as:

$$d_L = 20 \text{ in}$$

$$d_T = 15 \text{ in}$$

$$d_m = 1 \text{ in}$$

The muscle force is the only force resisting the tipping of the body about the fulcrum point on the lumbar spine. Therefore, balancing the moments about the spine yields:

$$M(1) = 50(20) + 120(15) = 2800 \text{ lb}$$

At first glance, this may seem to be an impossible load as it would indicate that the compression on the spine would be the sum of the weight lifted, the weight of the torso, and the muscle force, or combining to be almost 3,000 lb. Because of the short moment arm to the muscles, these loads are correct and have been verified by experiments. Very few people realize the loads that are placed on the skeletal system due to the fact the muscles get “the short end of the stick.”

The forearm provides another excellent example of this effect. Consider the forearm modeled as a simple lever as shown in **Figure 26**. A simple measurement on one's forearm will show that the length from the elbow to the palm of the hand is 8 to 10 times longer than the length from the elbow to the tendon attachment of the biceps. This means that if 25 lb are held in the palm of the hand, the muscle force must be between 200 and 250 lb. The compression on the elbow joint $C = M - W$ would be between 175 and 225 lb. It is easily seen that if the lever arm to the weight were increased with a tennis racket or a shovel, the compression on the joint would increase even more.

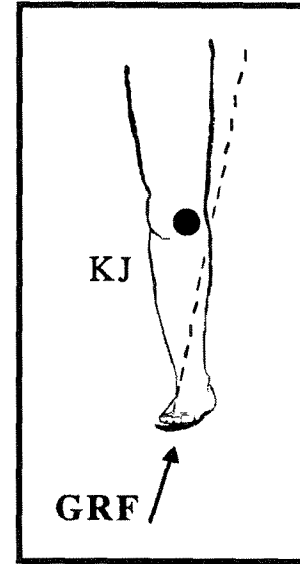


Figure 23.
Knee joint center and line of action of ground reaction force (GRF).

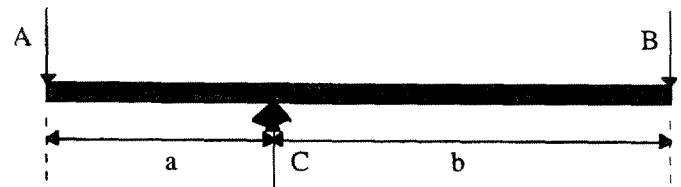


Figure 24.
Simple lever.

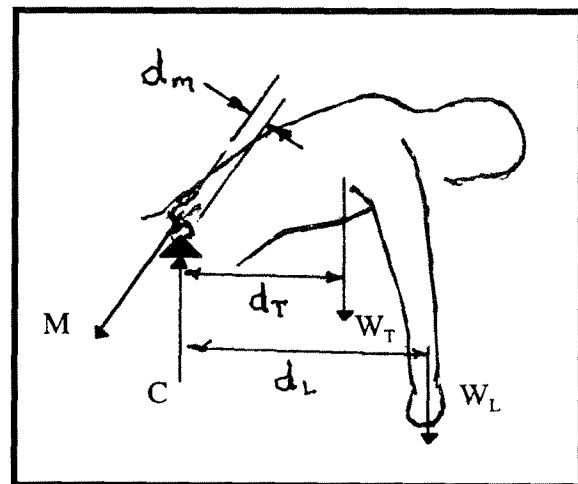


Figure 25
Lever model to determine lumbar spine load.

Muscle attachments are close to the joint centers so that small contractions of the muscle can produce large movements at the end of the levers producing a mechanical advantage in the motion of the limbs. Almost all loads on the muscular skeletal system can be modeled and understood by simple levers. These concepts can be applied in exercise therapy, orthotics, and in the understanding of the causes of injury.

POWER

Examination of the power expended by the muscles during a particular activity is a new tool that is being applied to gait analysis. Power is a measure of the rate of doing work, which is the product of the force applied in a certain direction and the distance the object moves in that direction.

$$\text{Work} = F d \quad [17]$$

where F is the force and d is the distance the object moves in the direction of the force.

The power expended is the rate at which work is performed or the product of the force applied in a certain direction and the velocity of movement in that direction.

$$P = F v \quad [18]$$

where v is the velocity in the direction of the force. Power is measured in Watts or Newton meters per second ($N \cdot m/s$). A moment also does work when it rotates an object through an angle, and the power performed by the moment is the product of the moment and the angular velocity of the object. Consider the power expended by the biceps when the elbow is extended or flexed as shown in **Figure 27**. The muscle moment in both **Figure 27a** and **27b** is a flexion

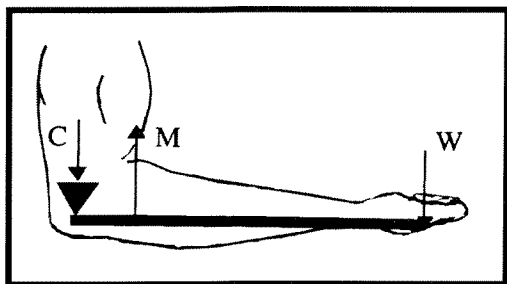


Figure 26.
Lever model of forearm.

moment but the arm is flexing in (a) and extending in (b). The power expended by the muscle in both cases is the product of the moment and the angular velocity of the forearm, but in case (a), the angular velocity is positive (in the same direction as the muscle moment), and in case (b), the angular velocity is negative (in the opposite direction of the muscle moment). The power in case (a) is positive and in case (b), it is negative. When examining the muscle activity, it is evident that in case (a), the muscle is doing concentric contraction, or positive work, and in case (b), the muscle is doing eccentric contraction (lengthening), or doing negative work.

Figure 28 shows the angle dorsiflexion and plantarflexion of the ankle joint during stance phase of gait where dorsiflexion is plotted positive, therein illustrating how the power can be used to understand the muscle activity. The ankle first plantarflexes as the GRF acts posterior to the ankle joint and then dorsiflexes as the center of mass passes over the foot and finally plantarflexes until toe-off. The muscle moment during stance phase is approximated by **Figure 29**. During the initial period of stance, the tibialis anterior is active as the foot is plantarflexing to foot-flat. During the rest of stance phase, the gastrocnemius muscles are active controlling the center of mass of the body as it passes over the foot and then providing the power to push off the body and transfer the weight to the opposite foot. The power of the muscles is shown in **Figure 30**. The initial power is negative as the tibialis anterior muscles break the foot during foot-fall and the power is again negative as the ankle plantar flexors control the dorsiflexion of the foot. The final power is positive as the plantar flexors go into concentric contraction to power the body up and forward.

Overuse injuries are usually associated with positive power output by the muscles (i.e., when the muscles are being used to produce positive work on the body). Examples of this are pushing off while running, jumping, rising during squatting, and other concentric contractions of the muscles. Trauma injuries usually occur when the power of the muscles is negative or the muscles are trying to break an external moment that is being applied. A common example of this is when a runner hits a pothole in the road and the GRF occurs on the forefoot instead of the heel. The plantar flexors are forced to try to resist a suddenly applied dorsiflexion moment, usually of a high magnitude applied at a rapid rate, and the heel cord cannot

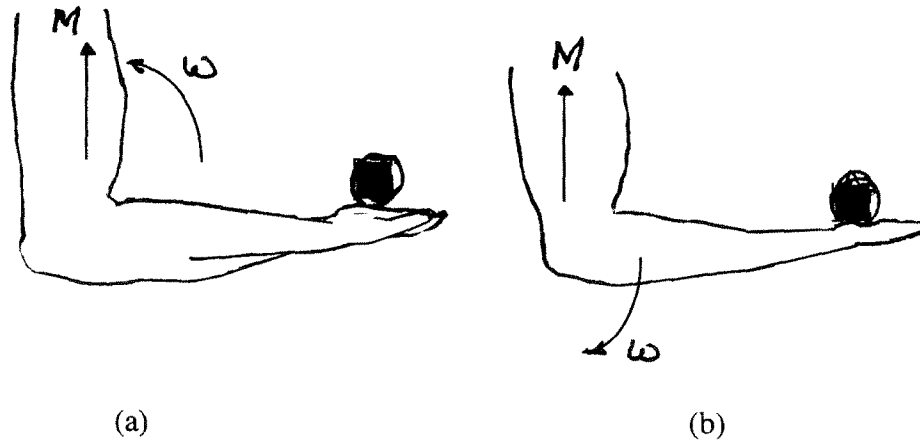


Figure 27.
Muscle power during elbow flexing or extending.

withstand that high strain rate, resulting in a partial tear or complete rupture.

APPLICATIONS OF MOTION ANALYSIS AND BIOMECHANICS

The applications of biodynamics to the medical field are increasing as research in this area is expanded and new equipment becomes available. The overall purpose of biodynamics is to provide a quantitative measurement of the function/dysfunction of the neuromuscular skeletal system. It is the responsibility of the biomechanist in cooperation with the clinician to provide information that cannot be obtained by other methods and, more importantly, to establish the clinical relevance of this information.

The most common application of motion analysis and biomechanics is gait analysis; for this reason, most clinical and research laboratories are called gait laboratories. However, to limit the application of this equipment and the analytical tools to gait analysis would be a failure to understand the full range of medical applications. One common application is the assessment of postural balance. Although balance is understood in a lay sense as the ability to maintain physical equilibrium, it is necessary to define it in a mathematical sense if biomechanical measurements are being made. When standing quietly, an individual is said to be in perfect balance when the center of gravity (c.g.) of the body is

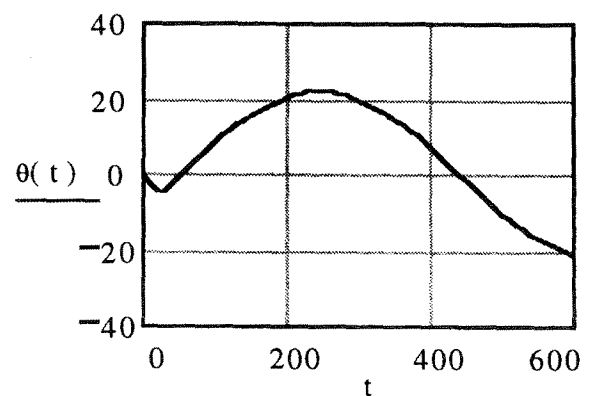


Figure 28.
Ankle dorsi/plantar flexion angular position.

directly over the center of pressure (COP) of the GRF. This is illustrated in **Figure 31**. The COP is measured with the force plate and can be accurately determined at any instant of time. The difficulty in obtaining rapid balance assessments is due to the inability to define the location of the center of mass in real time. An 11-segment model of the body may be made comprising the head, trunk, two upper arms, two forearms, pelvis, two thighs, and two lower legs. Data are available for the proportion of mass of each segment and the location of the center of mass of each segment for men and women of different sizes. However, accurate establish-

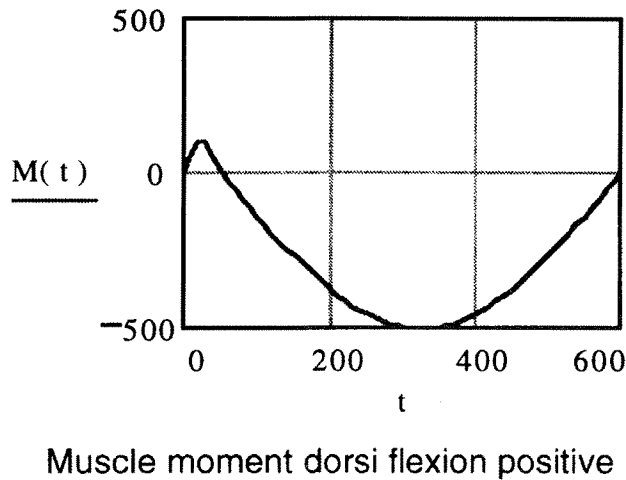


Figure 29.
Ankle muscle moment.

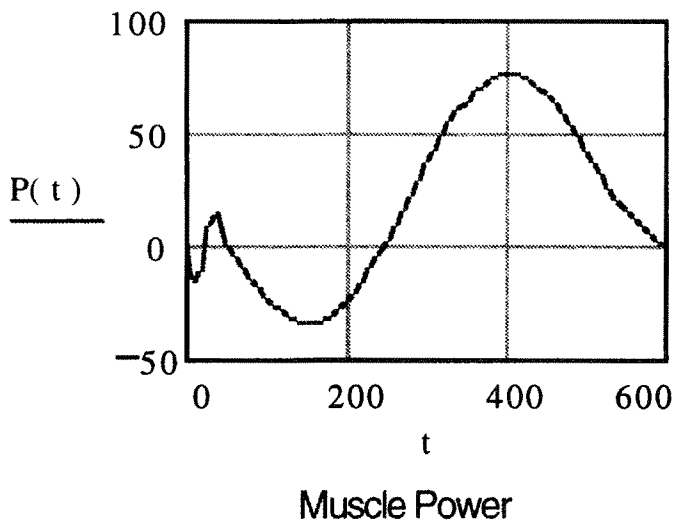


Figure 30.
Ankle muscle power.

ment of the position of each of these segments requires three markers per segment, totaling 33 markers.

The most common protocol to measure postural stability uses only a force plate. The COP is measured over a specific time frame, usually 20 seconds, and data are sampled at a specified rate, that is, 50 to 100 Hz. The resulting plot of the COP is called a stabilogram (see example in **Figure 32**).

The mean radius of the stabilogram can be computed and the velocity of the movement of the COP determined. These have been used as measures of

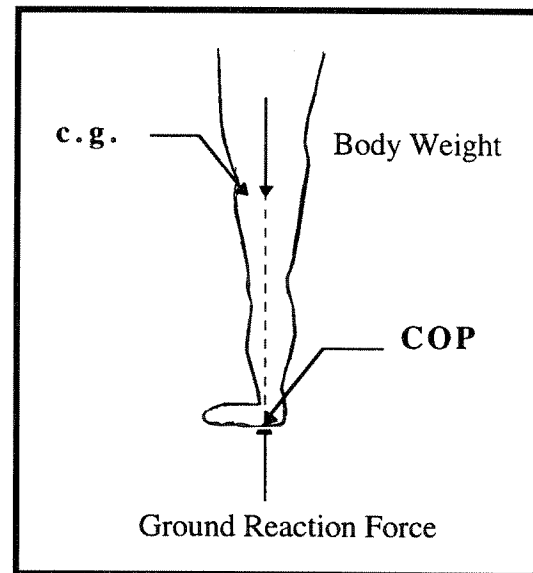


Figure 31.
Postural balance model.

postural stability. The COP must remain within the area of the base of support (the area underneath and between the feet), which decreases as the stance width decreases and increases as the feet are moved farther apart to a more stable position. Data have been collected for individuals standing with feet together, feet apart, feet tandem, or standing on one leg. In addition, eyes open and eyes closed data give the influence of vision on postural stability. Some laboratories have had the individual stand on soft mats to obtain information on proprioceptor influence on balance.

The major difficulty in using only the COP as a measure of balance is that the subject can move the position of the COP anteriorly, posteriorly, or laterally and still remain in a controlled balance position. Therefore, the data are dependent upon the individual trying to maintain balance and not deliberately perturbing the stabilogram. This is not the case when the difference between the c.g. and the COP is used as the measure of balance. Simpler models to determine the c.g. of the body are being introduced to obtain better measurement of postural balance and still maintain a workable laboratory protocol.

The ultimate goal of biodynamics is the development of predictive computer models for the neuromuscular skeletal system. This would allow the evaluation of an individual using the techniques of the indirect

dynamics model to determine joint motion and muscular activity. A computer model would then be created that could be driven using the muscle moments at the joints. The principal difficulty of models of this nature arises in the nonlinearity of the differential equations of motion. The solution of these equations becomes unstable as the solution progresses. Another problem is the over-determinacy of the number of muscle forces that act across a joint, that is, there are more flexors or extensors than are needed to flex or extend the joint. Using EMG, the temporal activity of these muscles may be determined but the reason for this over-determinacy is not fully understood. This problem is frequently approached using the mathematical methods of optimization.

In the simple model of the forearm shown in **Figure 33**, consider M_1 and M_2 as the forces in muscles 1 and 2 that flex the elbow. Either of these two flexors would be sufficient to flex the elbow or maintain equilibrium of the forearm when the weight W is applied. The equilibrium equation is

$$M_1 a + M_2 b = Wc \quad [19]$$

Note that the model of the forearm shown in **Figure 26** lumped the forces of the two muscles together as one equivalent muscle. Equation 19 is the only relevant equilibrium equation to determine both of the muscle forces, so there is no more information available from traditional biomechanics methods. EMG data will show that both of these muscles are active while holding the weight in the hand. Note that this model has been simplified and antagonistic muscle activity is not even considered.

Optimization techniques search for cost functions that should assume a minimal value to optimize the system. The earliest cost function that was introduced to optimize joint function was the total muscle force active at any time, which is

$$M_T = M_1 + M_2 \quad [20]$$

Therefore, Equation 19 would have to be satisfied while the total muscle force was minimized. This can be illustrated in **Figure 34**, where the total muscle force is plotted against the value of the two muscle forces (muscle space) and is shown as a shaded surface. Since the muscle forces must satisfy the equilibrium condition (Equation 19), the only solution values for the relative values of the muscle forces must lie on the line that represents that equation. Search along this line to find the point where the total muscle force is a minimum.

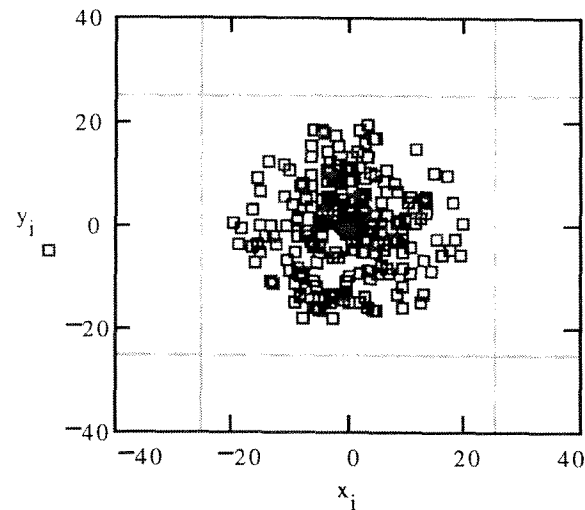


Figure 32.
Postural stabilogram.

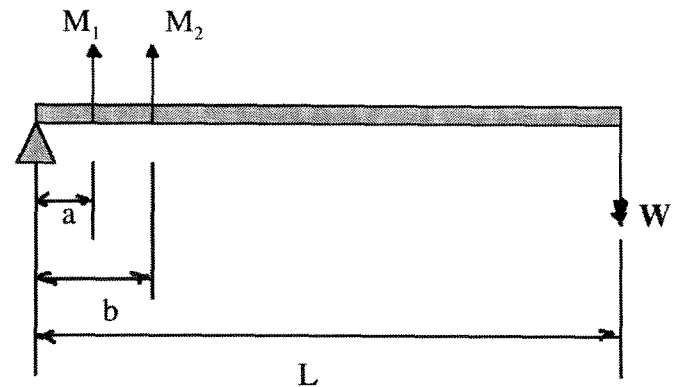


Figure 33.
Two muscle lever model of forearm.

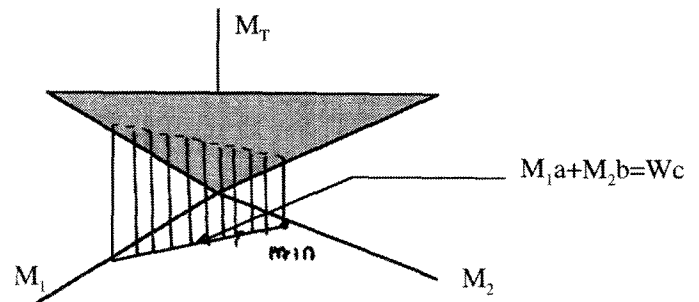


Figure 34.
Optimization of forearm muscles using a total muscle force cost function.

The optimum value of the muscle forces that minimize this cost function is such that M_1 would not be active and equilibrium would be maintained by use only of the muscle that had the largest moment arm or mechanical advantage. Experiments show that this is not the manner that the body uses to maintain equilibrium. Therefore, the cost function of the total muscle force is not the explanation of the over-employment of muscles during any given activity.

New cost functions have been investigated, such as the total muscle stress (muscle force divided by the cross-sectional area of the muscle), total muscle energy, and physiological fatigue of muscles. If an appropriate optimization model can be obtained, then the clinician can rehabilitate the patient in conjunction with the body's own attempt to minimize certain physiological costs.

Motion analysis and biomechanics are also currently being used to measure upper limb function, spinal curvature, and cervical spine movement. There are detailed studies to evaluate different orthopaedic surgeries, various instrumentation for total joint replacement, and to functionally evaluate different prosthetics and orthotics. Quantified functional assessment is also

valuable in evaluating pharmaceutical drugs used for muscular skeletal problems.

REFERENCES

1. Holden JP, Stanhope SJ, Orsini JA. Skeletal motion estimates: effect of surface target techniques. Proceedings of the Second World Congress of Biomechanics, Amsterdam, The Netherlands; 1994;(2):372.
2. Goldstein H. Classical mechanics. Reading, MA: Wesley Publishing Company; 1950. p. 144–8.
3. Grood ES, Suntay WJ. A joint coordinate system for the clinical description of three-dimensional motions. J Biomech Eng Trans ASME 1983;105:136–44.

ROBERT W. SOUTAS-LITTLE, Ph.D., is a Professor of theoretical mechanics and in the Division of Orthopaedic Surgery at Michigan State University. He is also the Director of the Biomechanics Evaluation Laboratory and the Biodynamics Research Laboratory. Dr. Soutas-Little has a B.S. in Mechanical Engineering from Duke University, an M.S. in Theoretical Mechanics from the University of Wisconsin, and a Ph.D. in Theoretical Mechanics with minors in physics and mathematics from the University of Wisconsin. He is the author of three books: *Elasticity*. New York: Prentice Hall, 1973; *Engineering Mechanics—Statics*. Prentice Hall, 1998; and *Engineering Mechanics—dynamics*. Prentice Hall, 1998; and has published over 100 articles in Journals and Proceedings.